

Supporting Material

Metal oxyhydroxide nanosheet assisted fabrication of ultrathin carbon molecular sieve membrane for hydrogen separation

Kaiqiang He^a, Yaoxin Hu^{b,}, Ze-Xian Low^a, Ruoxin Wang^a, Fanmengjing Wang^a, Hongyu*

Ma^a, Xiaofang Chen^a, Douglas R. MacFarlane^c, and Huanting Wang^{a,}*

^a Department of Chemical and Biological Engineering, Monash University, Clayton, Victoria 3800, Australia

^b Department of Civil Engineering, Monash University, Clayton, Victoria 3800, Australia

^c School of Chemistry, Monash University, Clayton, Victoria 3800, Australia

* Corresponding authors.

Email address: yaoxin.hu@monash.edu, huanting.wang@monash.edu

Figures

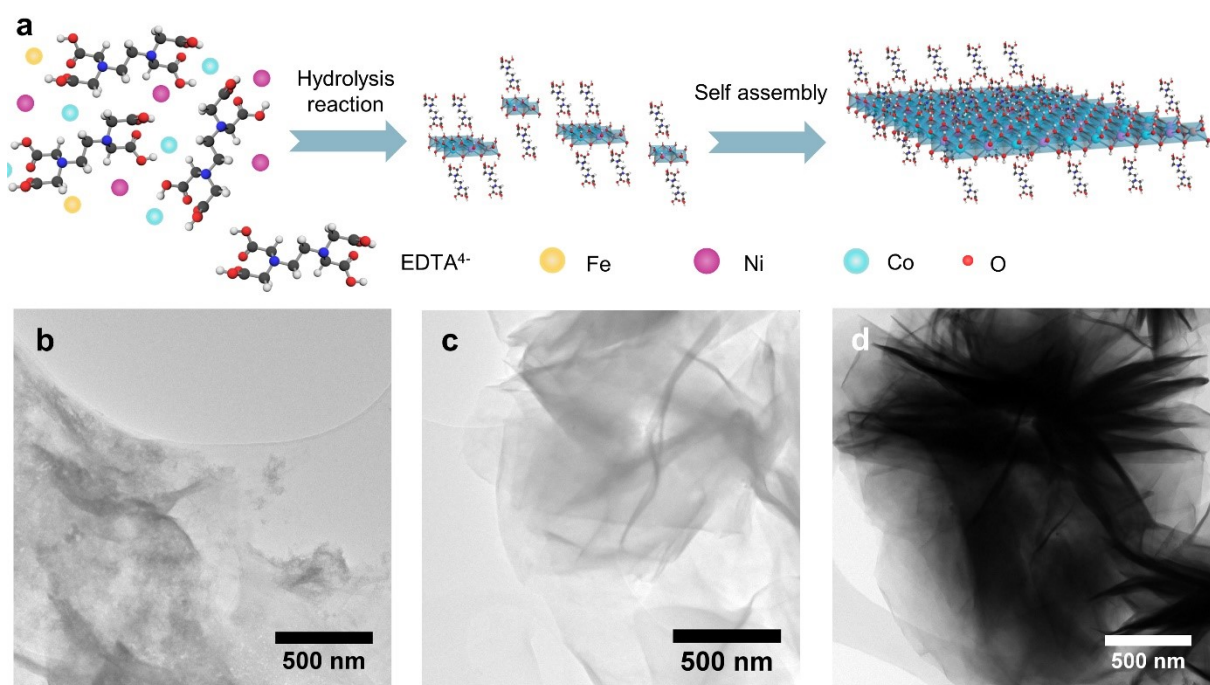


Fig. S1 (a) Schematic showing the production of FeCoNiOOH nanosheets via a surfactant-assisted self-assembly process; (b-d) TEM image of FeCoNiOOH nanosheets prepared with 3h, 6h and 12h, respectively.

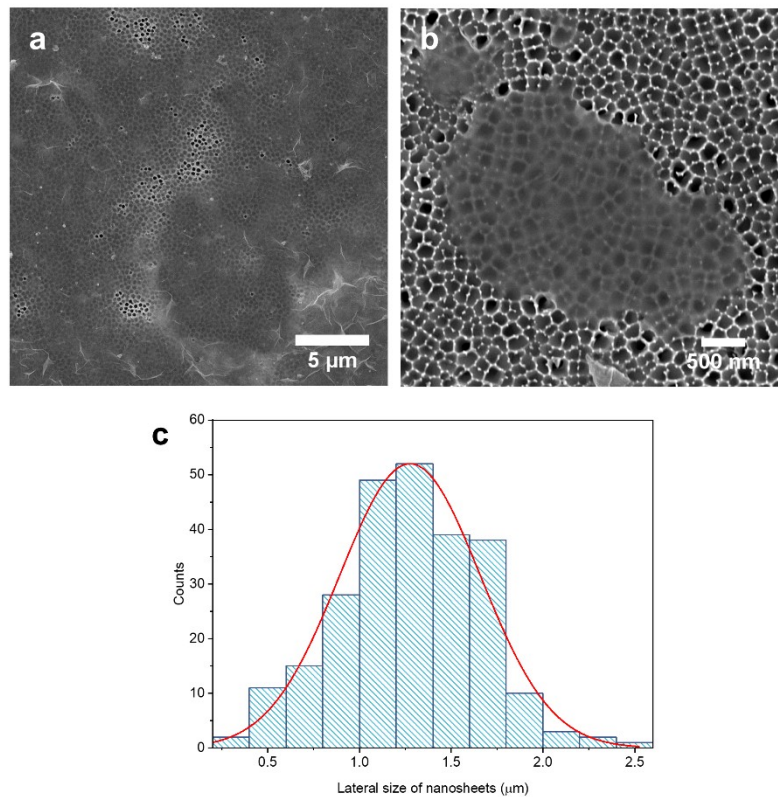


Fig. S2 (a-b) SEM images of the FeCoNiOOH nanosheets deposited on AAO; (c) Lateral size distribution of the nanosheets measured from SEM images over 250 nanosheets with a Gaussian fit.

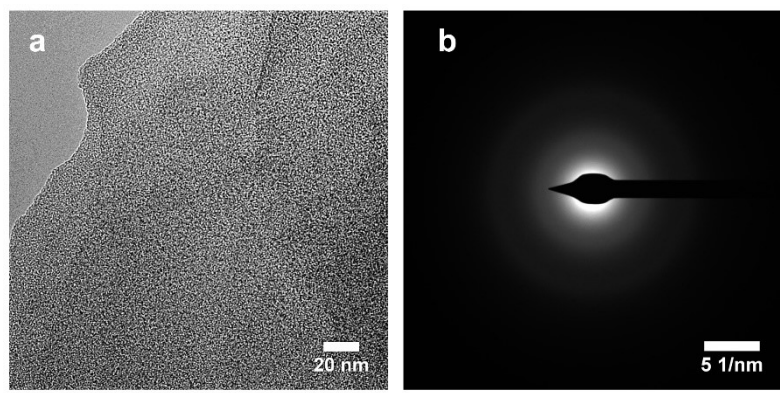


Fig. S3 (a) TEM image and (b) Corresponding selected area electron diffraction pattern at the edge of an ultrathin FeCoNiOOH nanosheet.

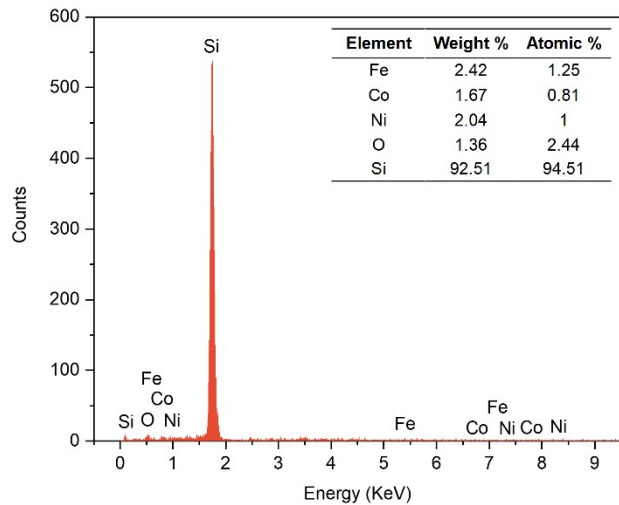


Fig. S4 SEM EDX spectrum of the FeCoNiOOH nanosheets deposited on a Si substrate with the relevant table of element component inserted. (The sharp peak of Si showing in the EDX spectrum is attributed to the Si substrate for depositing the nanosheets.)

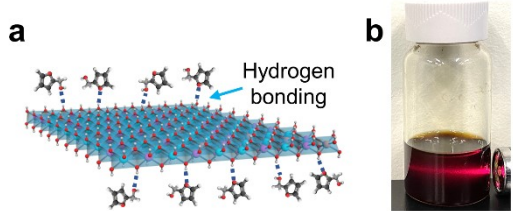


Fig. S5 (a) Schematic of the hydrogen bonding formed between furfuryl alcohol molecules and FeCoNiOOH nanosheet; (b) Tyndall effect of the nanosheets dispersed in furfuryl alcohol.

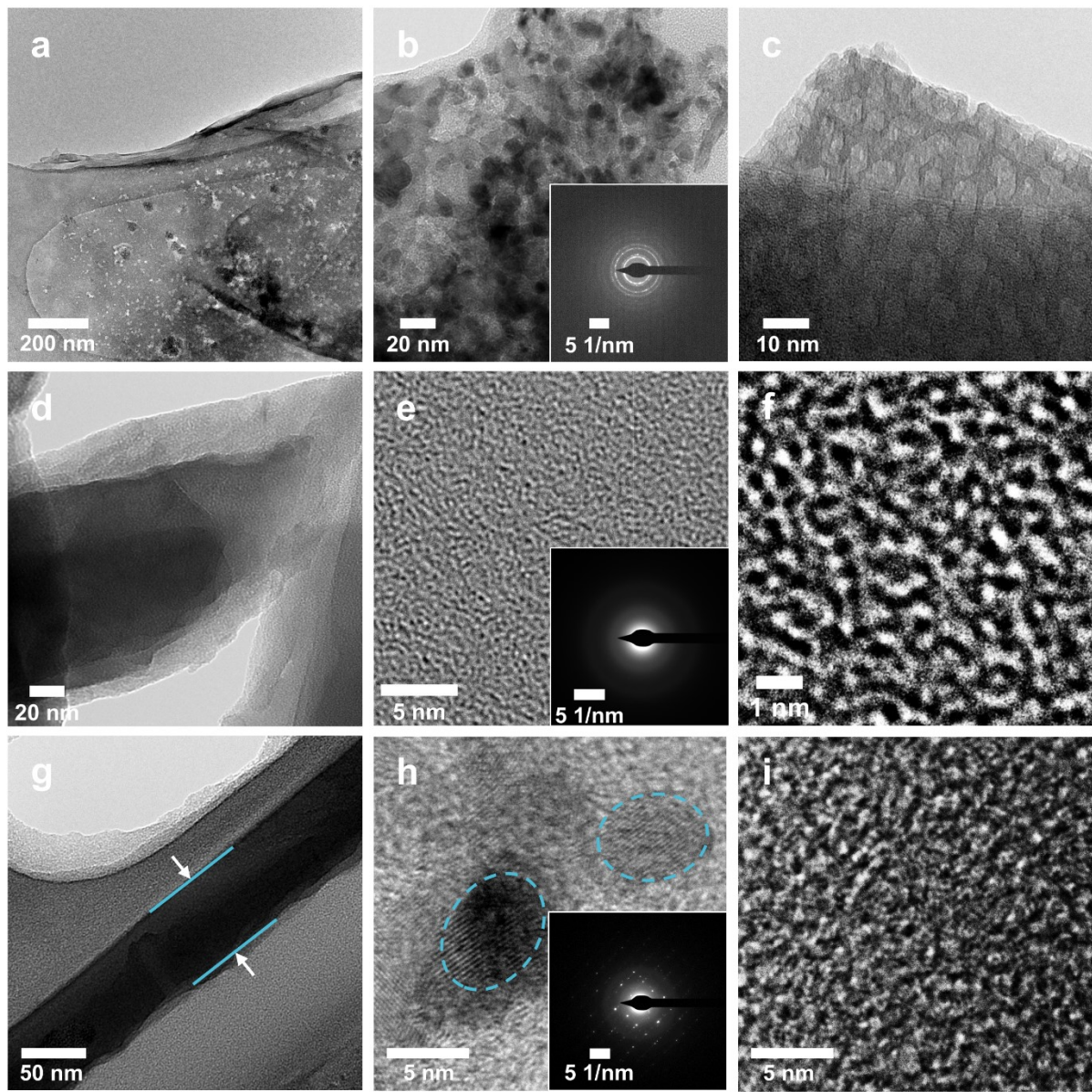


Fig. S6 (a-c) TEM characterization of FeCoNiOOH nanosheets after pyrolysis at 400 °C: (a) TEM image of the decomposed nanosheets showing generated nanopores and nanoparticles; (b) TEM image of the decomposed nanosheets showing numerous nanoparticles with corresponding SAED pattern inserted; (c) HRTEM image of the decomposed nanosheets showing nanoporous structure. (d-f) TEM characterization of PFA after pyrolysis at 450 °C: (d) TEM image of the carbonized PFA; (e) HRTEM image of the carbonized PFA with corresponding SAED pattern inserted; (f) Locally magnified HRTEM image of the carbonized PFA showing random packing of carbon plates and clusters. (g-i) TEM characterization of the

FeCoNiOOH nanosheets/PFA derived CMS membranes pyrolyzed at 450 °C: (g) TEM image of the CMS membrane cross-section; (h) HRTEM image of the nanoparticles shown in the CMS membrane due to the decomposition of the FeCoNiOOH nanosheets; (i) HRTEM image showing disordered pore structure of the carbon phase in the CMS membrane.

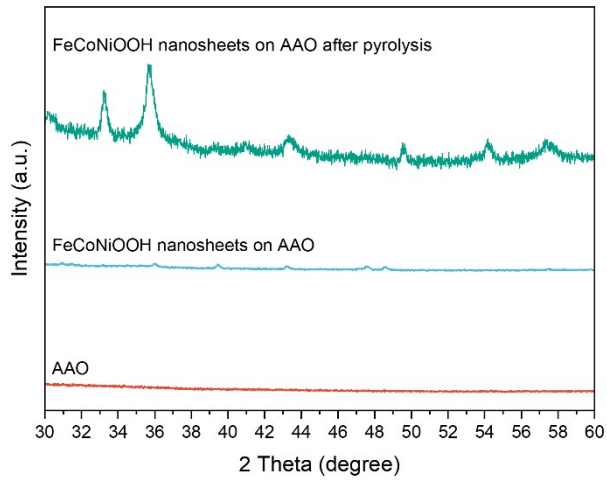


Fig. S7 XRD results of the AAO substrate, FeCoNiOOH nanosheets deposited on AAO before and after pyrolysis at 400 °C.

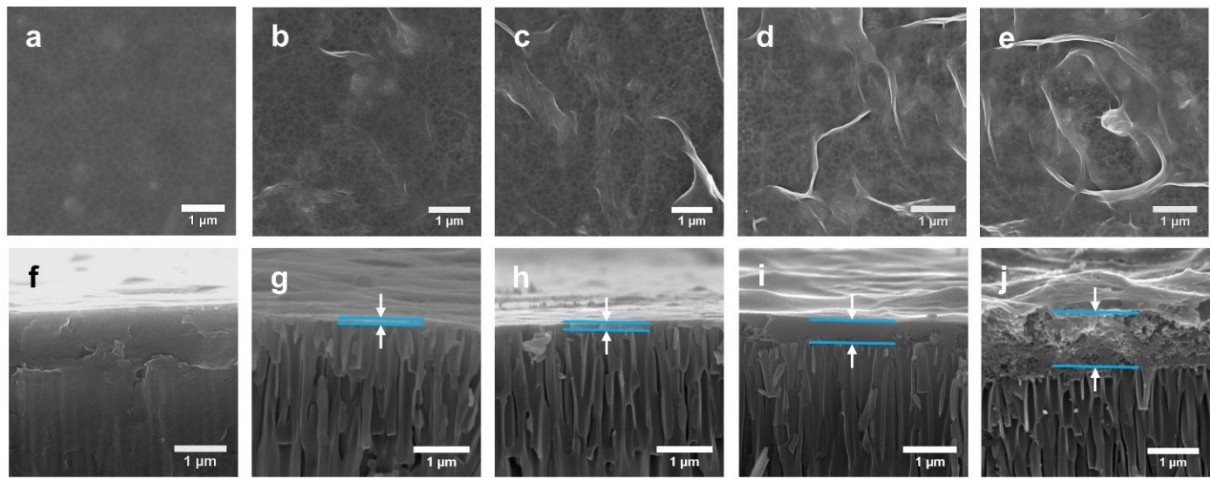


Fig. S8 SEM (a-e) surface and (f-j) cross-sectional images of FeCoNiOOH nanosheets/PFA based carbon membranes pyrolyzed under 525 °C with 0.9, 1.8, 3.5, 8.8 and 17.6 wt% of nanosheets loaded.

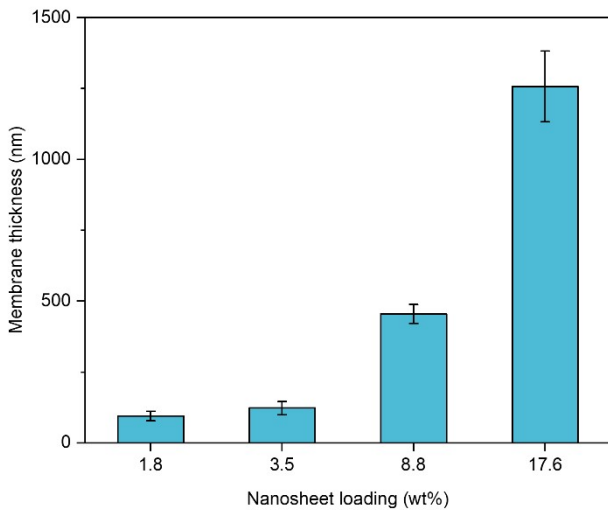


Fig. S9 Effective membrane thickness change of FeCoNiOOH nanosheets/PFA based carbon membranes with different nanosheets loading and pyrolyzed under 525 °C.

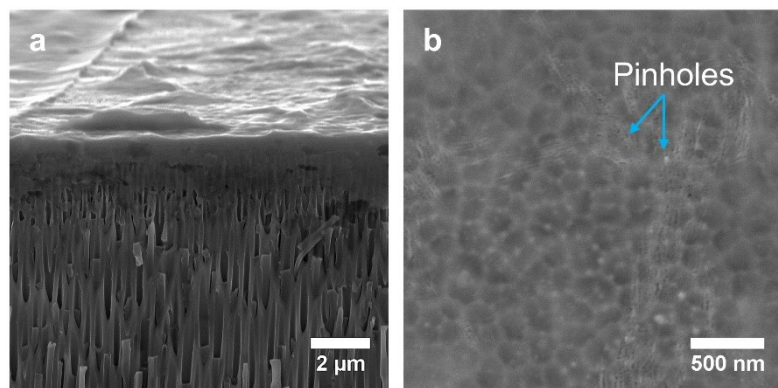


Fig. S10 (a) SEM cross-sectional image of 0.9 wt% FeCoNiOOH nanosheets/PFA based carbon membranes pyrolyzed under 525 °C presenting the infiltration of polymer into the AAO substrate owing to insufficient nanosheets introduced; (b) SEM surface image of 8.8 wt% FeCoNiOOH nanosheets/PFA based carbon membranes pyrolyzed under 525 °C showing the generation of pinholes when excessive amount of nanosheets incorporated.

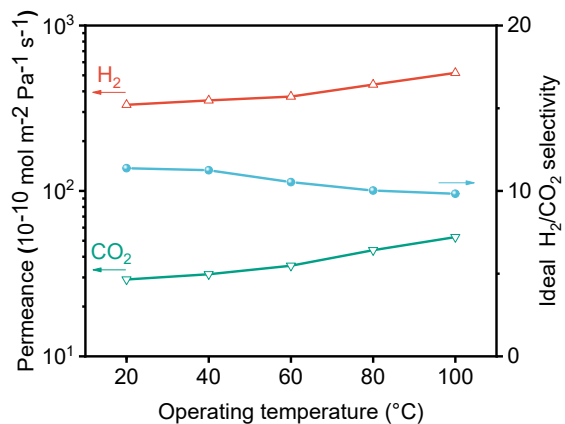


Fig. S11 The permeance and ideal selectivity as a function of permeation temperature from 20 to 100 °C for FeCoNiOOH nanosheet/PFA derived carbon membrane sample with 1.8wt% nanosheets pyrolyzed at 525 °C.

Table S1 Gas separation performance of MOOH nanosheet/PFA derived carbon membranes with a loading of 1.8 wt% of nanosheets pyrolyzed at different temperatures.

Carbonization temperature (°C)	H ₂ permeance (10 ⁻⁸ mol m ⁻² s ⁻¹ Pa ⁻¹)	H ₂ /N ₂ ideal selectivity	H ₂ /CO ₂ ideal selectivity
25	0.37	1.1	-
450	1.78	3	3.4
525	3.32	46	11.4
600	9.6	5.3	5.9

Table S2 Gas separation performance of MOOH nanosheet/PFA derived carbon membranes with different nanosheet loadings pyrolyzed at 525 °C.

Loading of MOOH nanosheets	Membrane thickness (nm)	H ₂ permeance (10 ⁻⁸ mol m ⁻² s ⁻¹ Pa ⁻¹)	Ideal selectivities			
			H ₂ /N ₂	H ₂ /CO ₂	H ₂ /CH ₄	H ₂ /O ₂
0.9	-[a]	0.26	4	5	3.1	-
1.8	95 ± 17	3.32	46	11.4	38.3	34.8
3.5	123 ± 23	7.88	4.2	4.4	3.1	-
8.8	455 ± 33	15.63	3.8	4.6	2.9	-
17.6	1257 ± 125	48	3.5	3.9	2.5	-

[a] The effective membrane thickness cannot be estimated here due to the polymer infiltration into the substrate.

Table S3 Gas separation performance of FeCoNiOOH nanosheet/PFA derived carbon membrane samples with 1.8wt% nanosheets pyrolyzed at 525 °C.

Sample	H ₂ permeance (10 ⁻⁸ mol m ⁻² s ⁻¹ Pa ⁻¹)	H ₂ /CO ₂ ideal selectivity	Average H ₂ permeance (10 ⁻⁸ mol m ⁻² s ⁻¹ Pa ⁻¹)	Average H ₂ /CO ₂ ideal selectivity
1	3.32	11.4		
2	2.71	9.3	2.78 ± 0.51	10.1 ± 1.1
3	2.31	9.7		

Table S4 Comparison of single-gas and mixed-gas permeation results for FeCoNiOOH nanosheet/PFA derived carbon membrane sample with 1.8wt% nanosheets pyrolyzed at 525 °C.

Tests	H ₂ permeance (10 ⁻⁸ mol m ⁻² s ⁻¹ Pa ⁻¹)	H ₂ /CO ₂ selectivity
Single-gas permeation	3.32	11.4
Mixed-gas permeation	3.2	10.5

Table S5 Permeance and selectivity at different permeation temperatures for the FeCoNiOOH nanosheet/PFA derived carbon membrane sample with 1.8wt% nanosheets pyrolyzed at 525 °C.

Permeation temperature (°C)	H ₂ permeance (10 ⁻⁸ mol m ⁻² s ⁻¹ Pa ⁻¹)	CO ₂ permeance (10 ⁻⁸ mol m ⁻² s ⁻¹ Pa ⁻¹)	H ₂ /CO ₂ ideal selectivity
20	3.32	0.29	11.4
40	3.53	0.31	11.3
60	3.72	0.35	10.5
80	4.4	0.44	10
100	5.17	0.53	9.83

Table S6 Comparison of gas separation performance for the MOOH nanosheet/PFA derived carbon membrane with carbon membranes produced with other methods.

Method	Precursor	Membrane	Pyrolysis	H ₂	H ₂ /CO ₂	Ref.
		thickness (μm)	temperature (°C)	permeance (GPU) ^[a]	ideal selectivity	
Dip coating	PFA	10	600	20.3	11	¹
Ultrasonic deposition	PFA	4.7	450	7.76	13.7	²
Vapour deposition	PFA	3.1	600	76.1	4.4	³
CNT scaffolding	PFA	0.32	500	56.4	5.9	⁴
Substrate transferring	Matrimid	0.1	500	761	1.53	⁵
2D templating	Polyimide	40	425	2.42	5.1	⁶
2D self-sacrificial templating	PFA	0.11	525	99.1	11.4	This work

[a] 1 GPU = 3.35×10^{-10} mol m⁻² s⁻¹ Pa⁻¹

Table S7 Comparison of gas separation performance for the MOOH nanosheet/PFA derived carbon membrane with different types of membranes.

Membranes	Membrane thickness (μm)	H ₂ permeance (GPU) ^[a]	H ₂ /CO ₂ ideal selectivity	References
ZIF-8 on polysulfone	3.6	1403	2.7	7
ZIF-8 on ammoniated PVDF	0.87	3552	3	8
ZIF-8 on layered double hydroxide (LDH) modified alumina	20	439	4.2	9
ZIF-8/Graphene oxide	0.1	163	1.6	10
ZIF-22 on titania	40	439	7.2	11
ZIF-7 on alumina	1.5	239	6.7	12
ZIF-90 on alumina	20	749	7.2	13
UiO-66/Poly(acrylic acid)	0.32	1.23	20.3	14
MOF-5/Matrimid	35	1.51	2.7	15
ZIF-8/Matrimid	40	0.446	3.8	16

ZSM-5/Matrimid	40	0.547	2.57	¹⁷
ZIF-8/ Polybenzimidazole s (PBIs)	5.88	64.5	12.3	¹⁸
ZIF-8/PBI hollow fiber membrane	0.307	107	16.1	¹⁹
Polyamide	0.2	25.8	14.3	²⁰
PBI on polyimide	0.1	48.5	33.3	²¹
Poly(benzoxazole- co-imide)	70	72.8	3.4	²²
m-PBI	20	23.9	24	²³
TADPS-IPA	21.5	14.9	19	²⁴
TADPS-TPA	19.5	19	13	²⁴
MOOH nanosheets / PFA derived carbon membrane	0.11	99.1	11.4	This work

[a] 1 GPU = 3.35×10^{-10} mol m⁻² s⁻¹ Pa⁻¹

References

- 1 C. Song, T. Wang, X. Wang, J. Qiu and Y. Cao, *Separation and Purification Technology*, 2008, **58**, 412–418.
- 2 M. B. Shiflett and H. C. Foley, *Journal of Membrane Science*, 2000, **179**, 275–282.
- 3 H. Wang, L. Zhang and G. R. Gavalas, *Journal of Membrane Science*, 2000, **177**, 25–31.
- 4 J. Hou, H. Zhang, Y. Hu, X. Li, X. Chen, S. Kim, Y. Wang, G. P. Simon and H. Wang, *ACS Appl. Mater. Interfaces*, 2018, **10**, 20182–20188.
- 5 S. Huang, L. F. Villalobos, D. J. Babu, G. He, M. Li, A. Züttel and K. V. Agrawal, *ACS Appl. Mater. Interfaces*, 2019, **11**, 16729–16736.
- 6 Y. Wang, Z.-X. Low, S. Kim, H. Zhang, X. Chen, J. Hou, J. G. Seong, Y. M. Lee, G. P. Simon, C. H. J. Davies and H. Wang, *Angewandte Chemie International Edition*, 2018, **57**, 16056–16061.
- 7 W. Li, Z. Yang, G. Zhang, Z. Fan, Q. Meng, C. Shen and C. Gao, *J. Mater. Chem. A*, 2014, **2**, 2110–2118.
- 8 W. Li, P. Su, Z. Li, Z. Xu, F. Wang, H. Ou, J. Zhang, G. Zhang and E. Zeng, *Nat Commun*, 2017, **8**, 406.
- 9 Y. Liu, N. Wang, J. H. Pan, F. Steinbach and J. Caro, *J. Am. Chem. Soc.*, 2014, **136**, 14353–14356.
- 10 Y. Hu, J. Wei, Y. Liang, H. Zhang, X. Zhang, W. Shen and H. Wang, *Angewandte Chemie International Edition*, 2016, **55**, 2048–2052.
- 11 A. Huang, H. Bux, F. Steinbach and J. Caro, *Angewandte Chemie*, 2010, **122**, 5078–5081.
- 12 Y.-S. Li, F.-Y. Liang, H. Bux, A. Feldhoff, W.-S. Yang and J. Caro, *Angewandte Chemie*, 2010, **122**, 558–561.
- 13 A. Huang, W. Dou and J. Caro, *J. Am. Chem. Soc.*, 2010, **132**, 15562–15564.
- 14 F. Xiang, A. M. Marti and D. P. Hopkinson, *Journal of Membrane Science*, 2018, **556**, 146–153.
- 15 E. V. Perez, K. J. Balkus, J. P. Ferraris and I. H. Musselman, *Journal of Membrane Science*, 2009, **328**, 165–173.
- 16 Ma. J. C. Ordoñez, K. J. Balkus, J. P. Ferraris and I. H. Musselman, *Journal of Membrane Science*, 2010, **361**, 28–37.
- 17 Y. Zhang, K. J. Balkus, I. H. Musselman and J. P. Ferraris, *Journal of Membrane Science*, 2008, **325**, 28–39.
- 18 T. Yang, G. M. Shi and T.-S. Chung, *Advanced Energy Materials*, 2012, **2**, 1358–1367.
- 19 M. Etxeberria-Benavides, T. Johnson, S. Cao, B. Zornoza, J. Coronas, J. Sanchez-Lainez, A. Sabetghadam, X. Liu, E. Andres-Garcia, F. Kapteijn, J. Gascon and O. David, *Separation and Purification Technology*, 2020, **237**, 116347.
- 20 Z. Ali, F. Pacheco, E. Litwiller, Y. Wang, Y. Han and I. Pinna, *J. Mater. Chem. A*, 2017, **6**, 30–35.
- 21 J. Sánchez-Láinez, M. Etxeberria-Benavides, O. David, C. Téllez and J. Coronas, *ChemSusChem*, 2021, **14**, 952–960.
- 22 C. Y. Soo, H. J. Jo, Y. M. Lee, J. R. Quay and M. K. Murphy, *Journal of Membrane Science*, 2013, **444**, 365–377.
- 23 K. A. Stevens, J. D. Moon, H. Borjigin, R. Liu, R. M. Joseph, J. S. Riffle and B. D. Freeman, *Journal of Membrane Science*, 2020, **593**, 117427.
- 24 H. Borjigin, K. A. Stevens, R. Liu, J. D. Moon, A. T. Shaver, S. Swinnea, B. D. Freeman, J. S. Riffle and J. E. McGrath, *Polymer*, 2015, **71**, 135–142.